Adsorption (2007) 13: 307–314
DOI 10.1007/s10450-007-9061-1

Pore accessibility of N_2 and Ar in disordered nanoporous solids: theory and experiment

T.X. Nguyen · S.K. Bhatia

Received: 20 April 2007 / Revised: 18 July 2007 / Accepted: 24 September 2007 / Published online: 16 October 2007

Abstract Recently (Nguyen and Bhatia, J. Phys. Chem. C 111:2212–2222, 2007) we have proposed a new algorithm utilising cluster analysis principles to determine pore network accessibility of a disordered material. The algorithm was applied to determine pore accessibility of the reconstructed molecular structure of a saccharose char, obtained in our recent work using hybrid reverse Monte Carlo simulation (Nguyen et al., Mol. Simul. 32:567–577, 2006). The method also identifies kinetically closed pores not accessed by adsorbate molecules at low temperature, when their low kinetic energy cannot overcome the potential barrier at the mouths of pores that can otherwise accommodate them.

In the current work, the results are validated by transition state theory calculations for N_2 and Ar adsorption, showing that N_2 can equilibrate in narrow micropores at practical time scales at 300 K, but not at 77 K. Large differences between time scales for micropore entry and exit are predicted at low temperature for N_2, the latter being smaller by over three orders of magnitude. For N_2 at 77 K the time constant for pore entry exceeds 3 hr., while for exit it is 134 days. At 300 K these values are smaller than 1 μs, indicating good accessibility at this temperature. These results are verified by molecular dynamics simulations, which reveal that while N_2 molecules enter and leave all pores frequently at 300 K, entry and exit events for apparently inaccessible pores are absent at 77 K. For Ar at 87 K better accessibility is evident for the saccharose char compared to N_2 at 77 K. This finding is now experimentally shown in this work by comparison of pore size distributions obtained from experimental nitrogen adsorption isotherms of nitrogen and argon at 77 K and 87 K.

Keywords Gas phase adsorption · Molecular modeling · Pore accessibility · Transition state theory

T.X. Nguyen · S.K. Bhatia (✉)
Division of Chemical Engineering, The University of Queensland, Brisbane, QLD 4072, Australia
e-mail: s.bhatia@eng.uq.edu.au

1 Introduction

The understanding of the microstructure of porous materials in terms of pore morphology and topology plays a key role in the quantitative prediction of adsorption equilibrium and dynamics. Furthermore, while the pore morphology dictates adsorption capacity, the pore topology, which contains ultramicropores whose size is near the molecular dimension, provides selective adsorption of specific species from its mixtures. Such ultramicropores are found in carbon molecular sieves (CMS), polymer derived CMS, coals, and dehydrated zeolites, which are widely utilized for gaseous mixture separation purposes. The CMS is more attractive due to the fact that their pore structure is easier to be precisely tailored by heat treatment.

In practice, ultramicropores in CMS are normally viewed as pore entrances connecting neighboring pore cavities, through which transport of adsorbates is experimentally observed as an activated diffusion process with strong temperature dependence and therefore pore accessibility. Although such strong temperature dependence of pore accessibility is experimentally observed (Maggs 1952, 1953; Bae and Bhatia 2006), its molecular level basis has been scarcely investigated in the existing literature. Such understanding has significance for enhancement of adsorption selectivity of CMS by temperature adjustment, especially for separation

of important mixtures of small molecules such as CO_2/CH_4, CO_2/H_2 or H_2/D_2, as well as accurate prediction of adsorption equilibrium and dynamics properties, and explanation of hysteresis in such materials. However, porous carbon materials are not normally crystalline, but contain significantly varying contents of amorphous matter. Such amorphous content inevitably leads to formation of complex pore networks for which characterization is practically a very challenging task.

Reverse Monte Carlo (RMC) (McGreevy and Putsai 1988) and hybrid reverse Monte Carlo (Opletal et al. 2002) techniques have recently emerged as promising methods that enable one to generate atomistic models of the microstructure of porous carbons (Thomson and Gubbins 2000; Nguyen et al. 2006; Jain et al. 2006). The reconstructed atomistic model is realistic, and permits the determination of pore accessibility in porous carbons (Nguyen and Bhatia 2007). Furthermore, similar to real porous carbons, the reconstructed atomistic microstructure also possesses a complex pore network that leads to difficulty in rigorous estimation of the adsorption isotherm using grand canonical Monte Carlo (GCMC) simulation. This is because adsorption in disconnected regions or closed pores also arises from insertion moves of the technique, which is unphysical. At the same time, the pore connectivity problem also causes difficulty in preparation of initial configurations for equilibrium molecular dynamics (EMD) simulation using GCMC simulation or random placement of adsorbate molecules in the reconstructed carbon structure model, as such methods do not distinguish between open and closed pore spaces. Consequently, the determination of pore accessibility also helps resolve the above issues.

In this work, we propose a new algorithm that groups molecules of a close packed adsorbed phase into continuous and disconnected clusters, from which pore network connectivity is determined. We apply the algorithm to analyze pore network connectivity of the reconstructed microstructure of a saccharose char, obtained in our recent work using hybrid reverse Monte Carlo simulation (Nguyen et al. 2006). Through this technique kinetically closed pores in the reconstructed microstructure were identified. Subsequently, this kinetic feature of the connectivity was further confirmed in the experimental adsorption time scale by estimation of the crossing time of a single particle through connected neighboring pores using transition state theory (TST), successfully employed by several researchers to predict self-diffusivity of gases in zeolite materials (Sholl and Fitchthorn 1997; Beerdsen et al. 2004). From the estimation of the crossing time, the problems arising from apparent pore-blocking effects are elucidated.

2 Experimental study

A glassy carbon (P3M), reported by Pérez-Mendoza et al. (2006), and activated carbon fiber ACF15, reported in our previous work (Nguyen and Bhatia 2005), were degassed at 300°C overnight prior to nitrogen and argon adsorptions at 77 K and 87 K. A Micromeritics ASAP 2010 volumetric adsorption analyzer was used to obtain nitrogen and argon adsorption data at 77 K and 87 K in these carbons.

3 Mathematical modeling

3.1 Determination of pore network connectivity

Our approach to determine pore connectivity analyzes the connectivity of the fluid phase in the model of the solid structure. Since temperature (i.e. kinetic energy) is the main factor responsible for pores being kinetically closed, our analysis is based on the persistence of this effect even at high densities corresponding to that of the liquid phase, i.e. when average intermolecular distance, $\bar{d}_a$, is approximately equal to the equilibrium separation, $2^{1/6}\sigma_f$, based on the Lennard Jones (LJ) pair potential (Nguyen et al. 2002). Here σ_f is the fluid LJ size parameter, or collision diameter. This assumption covers most practical applications of gas adsorption using porous carbons, and the high density phase obtained in this condition is considered here as the "close packed" phase. In particular, the close packed adsorbed phase of argon and nitrogen can be obtained using GCMC simulation at 77 K and 87 K respectively. For other cases, the position of the first peak of the pair distribution function of the adsorbed phase is used to identify if a close packed adsorbed phase is reached.

In our technique we first fill up all pore spaces in the solid structure, including closed pores, with fluid, to form a close packed phase. Subsequently, the structure of the fluid phase is analyzed to determine if the atomistic solid structure subdivides the guest molecules into discrete clusters. Such discrete clusters signify closed pores, and their absence is indicative of continuous open pore space. Consequently, the determination of pore network connectivity in the atomistic model of porous carbon structure is based on analysis of the continuity of the close packed adsorbed phase throughout the solid structure model. This approach is central to our proposed algorithm to determine the pore connectivity in porous carbons. The algorithm comprises of three principal steps to determine pore connectivity.

3.1.1 Filling all pore spaces of the solid structure with close packed adsorbate

This step is straightforwardly performed using the conventional GCMC simulation, and is common in studies of the

adsorption of confined fluids. In GCMC simulation, the chemical potential, μ, volume, V, and temperature, T, are kept invariant, while the number of particles, N, and associated configurational energy, E, are allowed to fluctuate. In the procedure, microstate configurations are generated through the well established Metropolis sampling scheme for three trial types: moving, creating, and deleting molecules. The probability for each trial type being accepted is given by Adams' algorithm (Adams 1975).

In order to obtain close packing of the adsorbed phase we simulate adsorption equilibrium at the condition of interest such that all the kinetically closed pores are detected at this condition. For distinguishing physically closed pores from kinetically closed pores the adsorption simulations are performed at a reasonably high temperature at which kinetically closed pores are absent. In the current work, the configuration of the adsorbed phase has been collected after every ten million GCMC steps to ensure that detection of closed pores is independent of the microstates. The total number of configurations used for every GCMC run is 60 million.

3.1.2 *Determination of all adsorbate clusters in the solid structure model*

In order to determine the clusters, the maximum intermolecular distance between two first nearest neighbor adsorbate molecules in the same adsorbed cluster, $RC_{[i][i]}$, and the minimum intermolecular distance between two adsorbate molecules in two separate adsorbate clusters, $RC_{[i][j]}$, must be assigned. Here indices i and j inside the square brackets denote clusters i and j. Clearly, $RC_{[i][j]}$ must be greater than $RC_{[i][i]}$ in order to obtain complete resolution among the clusters. For a close packed adsorbed phase, $RC_{[i][i]}$ and $RC_{[i][j]}$ are given as previously reported in our recent work (Nguyen and Bhatia 2007)

$$RC_{[i][i]} = 1.2225\sigma_f \tag{1}$$

$$RC_{[i][j]} = 2\sigma_{sf} \tag{2}$$

Further, largest molecular size of adsorbate, which ensures a complete resolution of two clusters, is given as

$$\sigma_f^{\max} = 4.495\sigma_s \tag{3}$$

Thus, if the carbon LJ collision diameter is chosen to be 0.34 nm, the value of $\sigma_f^{\max}$ is 1.5 nm. This upper limit of $\sigma_f^{\max}$ covers a wide range of molecules. In practice, large and complex molecules are normally modeled as an array of atom sites linked by chemical bonds.

Finally, we determined all the clusters in the close packed adsorbate phase, using the values of $RC_{[i][i]}$ and $RC_{[i][j]}$ given in (1) and (2), respectively. In particular, the structure of the close packed adsorbed phase is considered as a graph in which adsorbate molecules are vertices. Each vertex connects to its neighboring vertices determined using $RC_{[i][i]}$. The *Breadth-first search* algorithm (Cormen et al. 2001) was employed to traverse all distinct path ways connected to two arbitrary vertices. During this traversal visited vertices are marked to guarantee each path way is not repeatedly visited. Accordingly, two molecules are in the same cluster if there exists at least one path way to connect them. By this way, all the clusters are determined.

3.1.3 *Determination of continuity of each cluster throughout the structure*

After determination of all the adsorbate clusters in the carbon structure model as described above, the final step determines connectivity of these clusters, and subsequently the pore connectivity of the carbon structure. Due to the periodic boundary conditions (PBC) applied to the primitive unit cell the carbon structure model is considered as a periodic solid. However, instead of determining the pore connectivity in a periodic unit cell, we perform this task in a periodic supercell constructed from this primitive unit cell. The periodic supercell preserves exactly the pore connectivity feature of the periodic structure. However, the advantage of the periodic supercell over the periodic unit cell is that it explicitly considers structural properties across boundaries. In particular, the relationship between the position of particles in the periodic supercell, $\mathbf{r}_s$, and that in the periodic unit cell, $\mathbf{r}_u$, is given as

$$\mathbf{r}_s = \underline{\underline{\mathbf{L}}} \cdot (\mathbf{r}_u + \mathbf{n}) \tag{4}$$

where the matrix $\underline{\underline{\mathbf{L}}}$ represents the Bravais lattice vectors, defined by the three unit cell vectors $\mathbf{L}_x = [L_x, 0, 0]$, $\mathbf{L}_y = [0, L_y, 0]$, and $\mathbf{L}_z = [0, 0, L_z]$. Here L_x, L_y, L_z are the lengths in the three dimensions of the simulation box. $\mathbf{n}$ is a repeating vector, whose three components, n_x, n_y, and n_x, are integers. For the periodic solid, $n_{\{\}} = 0, 1$, without loss of generality.

Figures 2a, 2b illustrate a 2D periodic unit cell and the corresponding periodic supercell respectively. The portions with right slanted black stripes represent the solid phase, and balls depict adsorbate molecules of the close packed adsorbed phase. From these figures, it may be observed that *the number of adsorbate molecules in a cluster associated with a closed pore is invariant from the periodic unit cell to the periodic supercell, while that associated with open space is doubled from the periodic unit cell to the periodic supercell.* This observation is the key principle in determining pore network connectivity in the carbon structure model. Accordingly, the degree of connectivity of a pore space, N_f, is given as

$$N_f = \frac{N_s^{\{i\}}}{N_u^{\{i\}}} - 1 \tag{5}$$

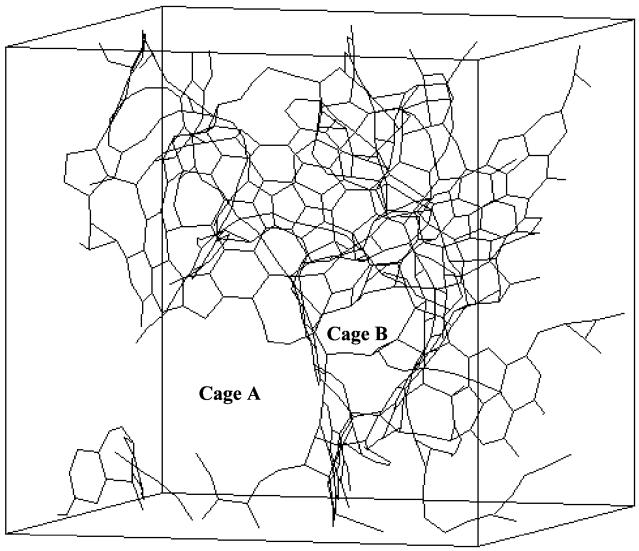

Fig. 1 Snapshot of converged configuration of activated saccharose char (Nguyen et al. 2006). *Cages A, B* depict the open and closed pore respectively, identified in Sect. 4.1

where $N_u^{\{i\}}$ and $N_s^{\{i\}}$ are the number of adsorbate molecules in the ith cluster in the periodic unit cell and in the periodic supercell respectively. Thus, a cluster is associated with a closed pore if N_f is equal to zero, and otherwise, to an open pore, for which N_f varies between unity and $(2^{\mathrm{d}} - 1)$. Here d is the number of dimensions in which periodic boundary conditions are imposed. Thus, for a 3-dimensional system, N_f can be as high as 7.

3.2 Transition state theory

Here we apply transition state theory, as described in our recent work (Nguyen and Bhatia 2007), to determine the crossing time of argon or nitrogen molecule from cage A to cage B or adsorption time, $\tau_{A\to B}$, and vice versa or desorption time, $\tau_{B\to A}$, in the atomistic structural model of saccharose char at low loading limit (Nguyen and Bhatia 2007). Cages A and B were identified in our recent work (Nguyen and Bhatia 2007) and are reproduced in Fig. 1 in this work. According to TST, the crossing time is given as

$$\tau_{A\to B} = \frac{1}{k_{A\to B}} \tag{6}$$

where $k_{A\to B}$ is a diffusion rate constant, given by TST [27–29] as

$$k_{A\to B} = \kappa\sqrt{\frac{k_B T}{2\pi m}}\frac{\int_{DS} e^{-\beta\phi_{sf}(\mathbf{r})}d^2\mathbf{r}}{\int_{V_{cageA}} e^{-\beta\phi_{sf}(\mathbf{r})}d^3\mathbf{r}} \tag{7}$$

Here κ is a transmission coefficient that represents the fraction of particles starting on top of the barrier with velocity towards cage B that successfully reach cage B, k_B is the Boltzmann constant, T is temperature and m is the mass of the particle. As previously shown (Nguyen and Bhatia 2007), κ is approximately about unity for N_2 and Ar. ϕ_{sf} is the interaction potential between the adsorbate particle i at position $\mathbf{r}$ and all solid atoms of the adsorbent phase, given as

$$\phi_{sf}(\mathbf{r}) = \sum_{j=1} u(|\mathbf{r}_j - \mathbf{r}|) \tag{8}$$

where u is the LJ (12-6) solid-fluid pair potential, given as

$$u(r) = 4\varepsilon_{sf}\left[\left(\frac{\sigma_{sf}}{r}\right)^{12} - \left(\frac{\sigma_{sf}}{r}\right)^{6}\right] \tag{9}$$

To evaluate the integral in the numerator of (7) we consider a small cubic box, which contains the dividing surface, of sufficiently small width, b, such that the energy landscape adjacent to the saddle point is similar for surfaces parallel to the diving surface. Here we assign b to be 0.1 Å. The integral term on the right hand side (R.H.S.) of (7) can be rewritten as

$$\frac{\int_{DS} e^{-\beta\phi_{sf}(\mathbf{r})}d^2\mathbf{r}}{\int_{cageA} e^{-\beta\phi_{sf}(\mathbf{r})}d^3\mathbf{r}} = \frac{1}{b}\frac{\int_{V_{box}} e^{-\beta\phi_{sf}(\mathbf{r})}d^3\mathbf{r}}{\int_{cageA} e^{-\beta\phi_{sf}(\mathbf{r})}d^3\mathbf{r}} \tag{10}$$

The two integrals in R.H.S. of (10) can be evaluated using Monte Carlo sampling integration (Press et al. 1986). Accordingly, (10) is rewritten for the case of one particle in cage A as

$$\frac{\int_{DS} e^{-\beta\phi_{sf}(\mathbf{r}')}d^2\mathbf{r}}{\int_{cageA} e^{-\beta\phi_{sf}(\mathbf{r})}d^3\mathbf{r}} = \frac{1}{b}\frac{\frac{V_{box}}{\tau'_{\max}}\sum_{n'=1}^{\tau'_{\max}} e^{-\beta\phi_{sf}(\mathbf{r}'_n)}}{\frac{V_{cageA}}{\tau_{\max}}\sum_{n=1}^{\tau_{\max}} e^{-\beta\phi_{sf}(\mathbf{r}_n)}} \tag{11}$$

where $\tau_{\max}$ and $\tau'_{\max}$ are the number of Monte Carlo (MC) trials. When the particle in the cage A falls in the dividing surface it is expected to vibrate around the saddle point of

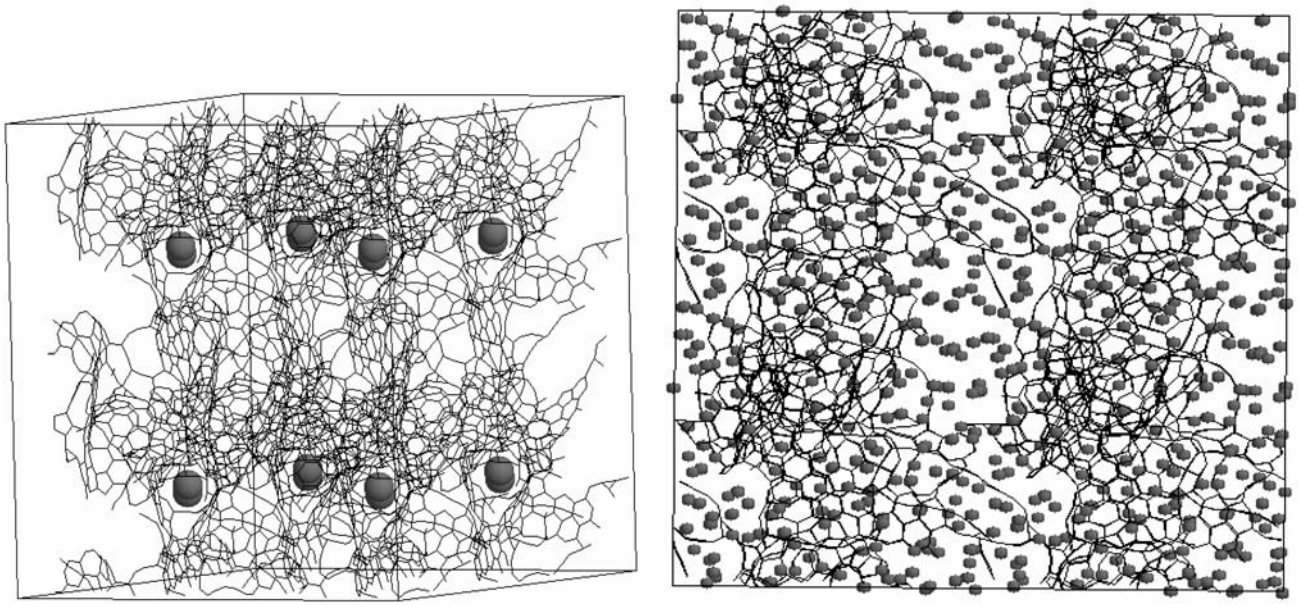

(a) (b)

Fig. 2 Illustration of clusters associated with **a** closed and **b** open pores in the periodic supercell at 77 K. In **a** there are kinetically closed pores that accommodate at maximum two nitrogen molecules

this surface due to extremely high energy around this saddle point. Accordingly, for sufficiently large number of MC trials, (11) can be equivalently expressed as

$$\frac{\int_{DS} e^{-\beta\phi_{sf}(\mathbf{r}')} d^2\mathbf{r}'}{\int_{cageA} e^{-\beta\phi_{sf}(\mathbf{r})} d^3\mathbf{r}} = \frac{1}{b} \frac{e^{-\beta\langle\phi_{sf}\rangle_{N,V_{box},T}}}{\sum_{n=1}^{\tau_{\max}} e^{-\beta\phi_{sf}(\mathbf{r}_n)}} \tag{12}$$

where $\tau_{\max}$ is the number of grid points in cage A, which is now approximately equal to the ratio of V_{cageA} to V_{box}. $\mathbf{r}_n$ is the coordinate of grid points in cage A. Thus, for a single particle the crossing time, $\tau_{A\to B}$, from cage A to cage B is finally obtained as

$$\tau_{A\to B} = \frac{b}{\kappa}\sqrt{\frac{2\pi m}{k_B T}} e^{\beta E_a} \tag{13}$$

where $\beta = \frac{1}{k_B T}$ and E_a is the effective activation energy, given as

$$E_a = \langle\phi_{sf}\rangle_{N,V_{box},T} + k_B T \ln\left(\sum_{n=1}^{\tau_{\max}} e^{-\beta\phi_{sf}(\mathbf{r}_n)}\right) \tag{14}$$

4 Results and discussion

All L-J parameters for argon, nitrogen, and carbon and implementation of the transition state theory to calculate the crossing time of argon and nitrogen were well presented in our recent work (Nguyen and Bhatia 2007). Here, we describe the main results of the calculated crossing time of nitrogen and argon through cages A and B in the atomistic structural model of saccharose char and experimental illustrations to support these calculated results.

4.1 Determination of pore connectivity in structural model of saccharose char

In this section, we apply our proposed algorithm to determine pore connectivity of the reconstructed microstructure model of a saccharose char, CS1000a, recently obtained using hybrid reverse Monte Carlo (HRMC) simulation (Nguyen et al. 2006), using nitrogen as probing molecule. At 77 K it has been found that there exists one closed pore space that accommodates at maximum of two nitrogen molecules, as shown in Fig. 2. From this figure, it can be seen that the detected closed pore is located in the interior of the unit cell. Accordingly, our previous replacement of the random insertion step used in GCMC simulation by local insertion at the simulation box surfaces (Nguyen et al. 2006) enables insertion of molecules in the open pore space. At the supercritical condition or 300 K, in order to obtain close packing of the adsorbed phase we performed GCMC simulations at very high fugacity ranging from 124,260 bar to 248,520 bar, and GCMC configurations were collected after every 10 millions of Monte Carlo (MC) steps. These GCMC configurations were then subjected to pore connectivity analysis using our proposed model. The results show that there is no physically closed pore space in this carbon

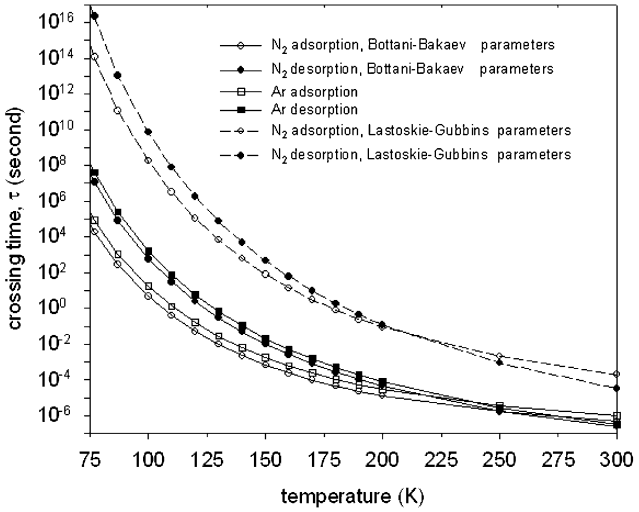

Fig. 3 Temperature variation of the estimated crossing time of a single nitrogen molecule (*circles*) and argon (*squares*) between cages A and B. For nitrogen, the crossing time is estimated using the LJ parameters given by Bottani and Bakaev (1994) (*solid line-circles*), and using the LJ parameters given by Lastoskie et al. (1993) (*dashed line-circles*)

structure at this temperature. Thus, there exists only a kinetically closed pore space detected in this carbon structure.

4.2 Investigation of the kinetic feature of connectivity using transition state theory

Figure 3 illustrates the crossing times $\tau_{A\to B}$ and $\tau_{B\to A}$ of N_2 and Ar from cage A to cage B and vice versa in the reconstructed model of saccharose char respectively, estimated using the transition state theory, as described in Sect. 3.2. A single center Lennard-Jones model of nitrogen was adopted, using the parameters reported by Bottani and Bakaev (1994). It was found that there are two dividing surfaces between cage A and cage B. The solid-fluid potential energy at the saddle point of the first dividing surface is about 183 kJ/mole, and that of the second dividing surface is about 3.5 kJ/mole. In this situation, the nitrogen molecule is not able to penetrate cage B from cage A, or vice versa, through the first surface at temperature below 300 K. Thus, the result of the crossing time was estimated for the second dividing surface with the lower value of the solid-fluid interaction potential at the saddle point, as shown in Fig. 3. The crossing times $\tau_{A\to B}$ and $\tau_{B\to A}$ can then be considered as the adsorption and desorption times respectively. From this figure it can be observed that the adsorption time below 72.1 K (>39 days) far exceeds the usual experimental adsorption time scale. In other words, cage B is essentially completely disconnected from cage A. The adsorption and desorption time at high temperatures (>150 K) is very short in comparison with that of collection of a single experimental adsorption point (30 minutes to a few hours), enabling attainment of equilibrium in the two cages. In other words, the total accessible volume of N_2 or adsorbed quantity increases in the high temperature range due to the complete connection between the two cages. Similar results are observed for argon. This finding was experimentally observed for carbon molecular sieves including naturally occurring MSC such as coals (Maggs 1952, 1953; Bae and Bhatia 2006).

It is interesting to see from Fig. 3 that the desorption time from cage B to cage A is much larger than the adsorption time, and well beyond the experimental adsorption time scale, at low temperatures below 87 K. This indicates a problem of obtaining actual adsorption equilibrium within this experimental time scale. In particular, while adsorption time of single nitrogen or argon molecule at 77 K (5–23 hours) lying within the experimental time scale, its desorption time (134–470 days) falls far beyond the practical time scale. Consequently, this leads to an open hysteresis loop or nitrogen entrapment in porous carbons. Such opened hysteresis loop was experimentally observed for nitrogen adsorption at 77 K in TCM 128 activated carbon by Koresh (1993).

From Fig. 3, it is also interesting to observe that the adsorption time of argon at 87 K (∼18 min) is considerably shorter than that of nitrogen at 77 K (>5 hours), as reported in our recent work (Nguyen and Bhatia 2007), although the adsorption time of these components are quite similar at the same temperature. Consequently, for systems similar to that investigated in this work adsorption equilibrium of argon at 87 K but not nitrogen at 77 K may be reached at practical time scales. In order to experimentally illustrate this case, we compare pore size distribution (PSD) extracted from experimental nitrogen and argon adsorption isotherms at 77 K and 87 K in a glassy carbon, reported by Pérez-Mendoza et al. (2006), and activated carbon fiber ACF15, reported in our previous work (Nguyen and Bhatia 2005). From Figs. 4a, 4b it can be observed that the pore size distribution of the glassy carbon probed by nitrogen and argon are very similar, especially the first peak, while the PSD of activated carbon fiber probed by nitrogen shows a shift to larger pore size compared with that probed by argon 87 K. This is likely due to much slower diffusion of nitrogen at low pressure which causes its measured filling pressure to exceed the actual equilibrium value. Such higher filling pressure gives rise to a shift of the first peak of PSD probed by nitrogen to larger pore size region. In order to further clarify this effect, we calculated adsorption isotherm of carbon dioxide at 323 K in these carbons using our proposed Finite Wall Thickness (FWT) model (Nguyen and Bhatia 2004), and their structural parameters (PSD and wall thickness distribution (PWTD)) extracted from argon at 87 K and nitrogen at 77 K, as depicted in Fig. 5. From this figure, it can be found that adsorbed quantity predicted by the use of structural parameters extracted from argon adsorption at 87 K at low pressure is consistently larger than that predicted by the use of structural parameters extracted from nitrogen adsorption at 77 K for both ACF 15 and P3M carbon samples. Such

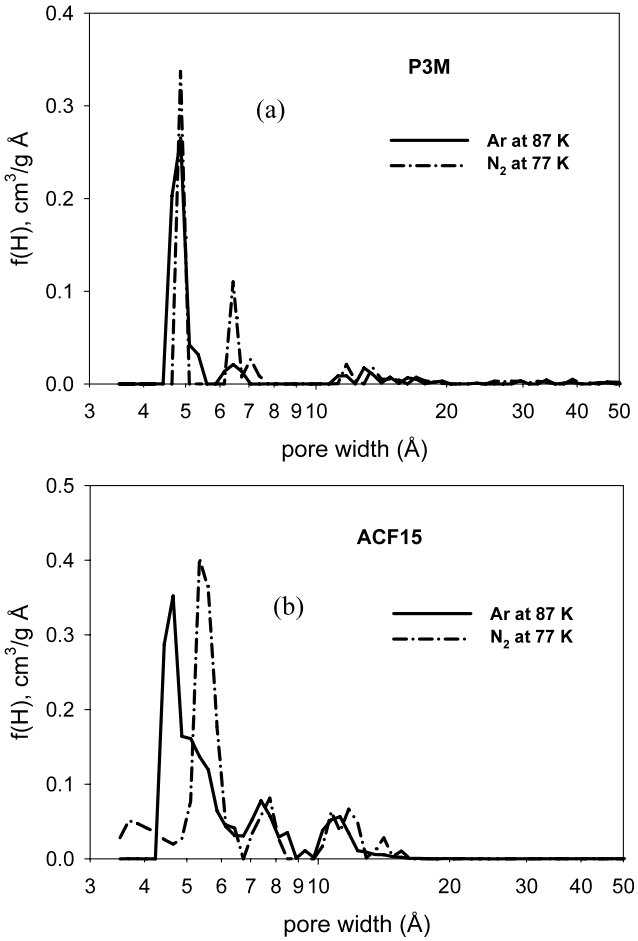

Fig. 4 Comparison of pore size distributions extracted from argon and nitrogen adsorptions at 87 K and 77 K in **a** glassy carbon (P3M), reported by Pérez-Mendoza (2006), and **b** activated carbon fiber ACF-15, reported in our previous work (Nguyen and Bhatia 2005), using the FWT mode (Nguyen and Bhatia 2004)

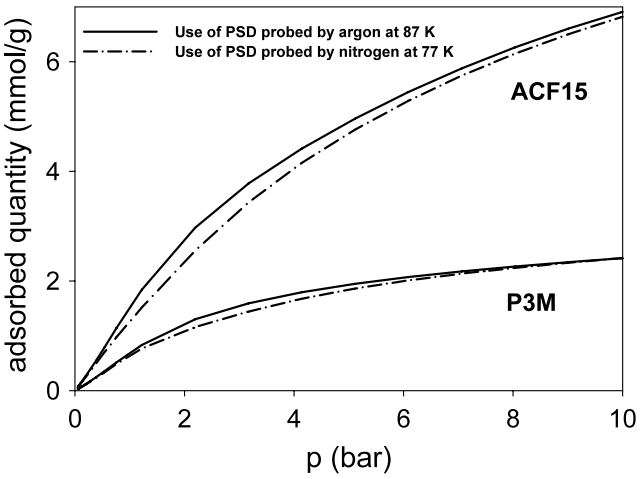

Fig. 5 Predicted adsorption isotherm of carbon dioxide at 323 K in the glassy carbon (P3M) and activated carbon (ACF-15) by the FWT model using structural parameters (PSD and PWTD) extracted from argon and nitrogen adsorptions at 87 K and 77 K

deviation can be significantly magnified if the size of pore mouth reduces, due to the effect on activation energy for the barrier crossing, in (14). This is readily seen by considering the ratio of the crossing time of argon at 87 K to that of nitrogen at 77 K, when activation energy E_a increases by δE_a due to reduction of the size of pore mouth. If we assume similar values of δE_a for nitrogen and argon, due to similarity of their solid-fluid interaction parameters (Nguyen and Bhatia 2007)

$$\left(\frac{\tau_{N_2 77K}}{\tau_{Ar87K}}\right)_{E_a+\delta E_a} = \left(\frac{\tau_{N_2 77K}}{\tau_{Ar87K}}\right)_{E_a} e^{\delta E_a/(k_B \Delta T)} \tag{15}$$

where effective temperature difference is given as

$$\Delta T = \frac{T_1 T_2}{[T_2(87K) - T_1(77K)]}$$

From the (15), it can be seen that the crossing time of nitrogen at 77 K increases exponentially faster than that of argon at 87 K when the size of pore mouth reduces. Consequently, the use of argon adsorption at 87 K provides more accurate characterization of microporous materials than the use of nitrogen adsorption at 77 K.

Finally, we compared the crossing time of nitrogen estimated using TST with that obtained using EMD simulation for the same LJ parameters at 300 K, prompted by the fact that the crossing time is within accessible MD time scales. We placed 5 nitrogen molecules in cage A, equivalent to approximately 3.2% in loading. It was found that the mean crossing time of nitrogen from cage A to cage B (455 ns) agrees very well with that estimated using the transition state theory (486 ns).

Before concluding, we now summarize the application of our proposed algorithm to obtain correct estimation of the adsorbed quantity, and self and corrected diffusivities in atomistic porous carbon models using the conventional GCMC and EMD simulations as follows. At any temperature, analysis of pore connectivity using our proposed algorithm is first performed to provide not only location of closed and open pores in the atomistic carbon model, but also coordinates of all the adsorbate molecules associated within these pore types. Subsequently, all the adsorbate molecules are then used as the basis set, as described above, to determine unphysically placed adsorbed molecules in the final configuration obtained using conventional GCMC simulation. The correct estimation of the adsorbed amount is then obtained by subtracting the unphysically placed molecules from the adsorbed amount obtained from the conventional GCMC simulation. The position of all the adsorbed molecules in the open pore spaces then provides a closed pore-free initial configuration for EMD simulation to obtain correct self and corrected diffusivities.

5 Conclusions

In this work, we presented the detailed description of our proposed algorithm based on cluster analysis of a close packed adsorbed phase to analyze the pore connectivity in atomistic structural models of porous carbons. The proposed algorithm has been shown to successfully probe the pore connectivity of a reconstructed structural model of saccharose char, obtained in our previous work using hybrid reverse Monte Carlo simulation (Nguyen et al. 2006), with nitrogen as the probing molecule. The result showed that there is no physically closed pore region in the atomistically reconstructed structure of saccharose char, but a kinetically closed pore space at 77 K. The finding of kinetically close pores in the atomistic structural model of saccharose char is confirmed by the EMD results. However, the same pore space does not appear kinetically closed to nitrogen at 300 K. This finding is further confirmed by estimation of the crossing time of nitrogen between detected open and closed pores using transition state theory. The results of the estimated crossing time and experimental adsorption data of nitrogen at 77 K and argon at 87 K, presented in this work, showed that argon adsorption at 87 K more accurately probes pore volume of microporous carbons than nitrogen at 77 K. Finally, our proposed algorithm is also applicable to other porous materials besides carbon such as zeolites, metal organic framework (MOF), porous silica glasses, providing the condition that the largest distance of the first nearest neighbors, $RC_{[i][i]}$, within a cluster is smaller than the smallest distance between two disconnected clusters, $RC_{[i][j]}$, as described in our algorithm, can be met.

Acknowledgements This research has been supported by a grant from the Australian Research Council, under the Discovery scheme, and a University of Queensland New Staff Research Start-up grant.

References

Adams, D.J.: Grand Canonical ensemble Monte Carlo for a Lennard-Jones fluid. Mol. Phys. **29**, 307–311 (1975)

Bae, J.-S., Bhatia, S.K.: High-pressure adsorption of methane and carbon dioxide on coal. Energy Fuel **20**, 2599–2607 (2006)

Beerdsen, E., Smit, B., Dubbeldam, D.: Molecular simulation of loading dependent slow diffusion in confined systems. Phys. Rev. Lett. **93**, 248301 (2004)

Bottani, E.J., Bakaev, V.A.: The Grand canonical ensemble Monte Carlo simulation of nitrogen in graphite. Langmuir **10**, 1550–1555 (1994)

Cormen, T.H., Leiserson, C.E., Rivest, R.L., Stein, C.: Introduction to Algorithms, 2nd edn. MIT Press, Cambridge (2001)

Jain, S.K., Gubbins, K.E., Pellenq, R.J.-M., Pikunic, J.P.: Molecular modeling and adsorption properties of porous carbons. Carbon **44**, 2445–2451 (2006)

Koresh, J.E.: On the flexibility of the carbon skeleton. J. Chem. Soc. Faraday Trans. **89**, 935–937 (1993)

Lastoskie, C., Gubbins, K.E., Quirke, N.: Pore size distribution analysis of microporous carbons: a density functional theory approach. J. Phys. Chem. **97**, 4786–4796 (1993)

Nguyen, T.X., Bhatia, S.K.: Probing the pore wall structure of nanoporous carbons using adsorption. Langmuir **20**, 3532–3535 (2004)

Nguyen, T.X., Bhatia, S.K.: Characterization of activated carbon fibers using argon adsorption. Carbon **43**, 775–785 (2005)

Nguyen, T.X., Bhatia, S.K.: Determination of pore accessibility in disordered nanoporous materials. J. Phys. Chem. C **111**, 2212–2222 (2007)

Nguyen, T.X., Bhatia, S.K., Nicholson, D.: Close packed transitions in slit-shaped pores: Density functional theory study of methane adsorption capacity in carbon. J. Chem. Phys. **117**, 10827–10836 (2002)

Nguyen, T.X., Bhatia, S.K., Jain, S.K., Gubbins, K.E.: Structure of saccharose-based carbon and transport of confined fluids: hybrid reverse Monte Carlo reconstruction and simulation studies. Mol. Simul. **32**, 567–577 (2006)

Maggs, F.A.P.: Anomalous adsorption of nitrogen at 90 °K. Nature **169**, 793–794 (1952)

Maggs, F.A.P.: Reversal of temperature dependence for physical adsorption of nitrogen. Res. Corresp. **6**, 13S–14S (1953)

McGreevy, R.L., Putsai, L.: Reverse Monte Carlo simulation: a new technique for the determination of disordered structures. Mol. Simul. **1**, 359–367 (1988)

Opletal, G., Petersen, T., O'Malley, B., Snook, I., McCulloch, D.G., Marks, N.A., Yarovsky, I.: Hybrid approach for generating realistic amorphous carbon structure using Metropolis and reverse Monte Carlo. Mol. Simul. **28**, 927–938 (2002)

Pérez-Mendoza, M., Schumacher, C., Suárez-García, F., Almazán-Almazán, M.C., Domingo-García, M., López-Garzón, F.J., Seaton, N.A.: Analysis of the microprous texture of a glassy carbon by adsorption measurements and Monte Carlo simulation. Evolution with chemical and physical activation. Carbon **44**, 638–645 (2006)

Press, W.H., Flannery, B.P., Teukolsky, S.A., Vetteling, W.T.: Numerical Recipes: The Art of Scientific Computing. Interscience, New York (1986)

Sholl, D.S., Fitchthorn, K.A.: Concerted diffusion of molecular clusters in a molecular sieve. Phys. Rev. Lett. **79**, 3569–3572 (1997)

Thomson, K.T., Gubbins, K.E.: Modelling structural morphology of microporous carbons by reverse Monte Carlo. Langmuir **16**, 5761–5773 (2000)